Williamson-Hall analysis in estimation of lattice strain in nanometer-sized ZnO particles

VD Mote[1], Y Purushotham[2] and BN Dole[1*]

Abstract

ZnO nanoparticles were prepared by coprecipitation method at 450°C. X-ray diffraction result indicates that the sample is having a crystalline wurtzite phase. Transmission electron microscopy (TEM) result reveals that the ZnO sample is spherical in shape with an average grain size of about 50 nm. X-ray peak broadening analysis was used to evaluate the crystalline sizes and lattice strain by the Williamson-Hall (W-H) analysis. All other relevant physical parameters such as strain, stress, and energy density values were also calculated using W-H analysis with different models, *viz*, uniform deformation model, uniform deformation stress model and uniform deformation energy density model. The root mean square strain was determined from the interplanar spacing and strain estimated from the three models. The three models yield different strain values; it may be due to the anisotropic nature of the material. The mean particle size of ZnO nanoparticles estimated from TEM analysis, Scherrer's formula and W-H analysis is highly intercorrelated.

Keywords: Nanostructured materials, Chemical synthesis, Crystal structure, TEM, W-H analysis

PACS: 81.07.-b, 81.07.Bc, 68.37.-d, 68.37.Lp, 73.63.Bd

Background

Semiconductor research is a very important field in the ongoing research activity across the world. As the semiconductor particles exhibit size-dependant properties like scaling of the energy gap and corresponding change in the optical properties, they are considered as the front runners in the technologically important materials. Zinc oxide is a II-VI semiconductor with a large bandgap ($E_g = 3.37$ eV) and high exciton binding energy (60 meV). It is widely used in a number of applications like photocatalysis, gas sensors, varistors, and low-voltage phosphor materials [1-4]. ZnO is the richest family of nanostructures among all semiconducting materials, both in structures and in properties due to its unique properties [5,6].

A perfect crystal would extend in all directions to infinity, so no crystals are perfect due to their finite size. This deviation from perfect crystallinity leads to a broadening of the diffraction peaks. The two main properties extracted from peak width analysis are (a) crystallite size and (b) lattice strain. Crystallite size is a measure of the size of a coherently diffracting domain. The crystallite size of the particles is not generally the same as the particle size due to the presence of polycrystalline aggregates [7]. The most common techniques used for the measurement of particle size rather than the crystallite size are BET, light scattering, scanning electron microscopy, and transmission electron microscopy (TEM) analysis. Lattice strain is a measure of the distribution of lattice constants arising from crystal imperfections, such as lattice dislocation. The other sources of strain are the grain boundary triple junction, contact or sinter stresses, stacking faults, coherency stresses, etc. [8]. X-ray line broadening is used for the investigation of dislocation distribution.

Apart from crystallite size reduction and alloying, mechanical alloying induces a large amount of strain in the powders [9]. X-ray profile analysis is a simple and powerful tool to estimate the crystallite size and lattice strain [10]. Among the available methods to estimate the crystallite size and lattice strain are the pseudo-Voigt function, Rietveld refinement, and Warren-

* Correspondence: dolebn_phys@yahoo.in
[1]Department of Physics, Materials Research Laboratory, Dr. Babasaheb Ambedkar Marathwada University, Aurangabad 431 004, India
Full list of author information is available at the end of the article

Averbach analysis [11-13]. Williamson-Hall (W-H) analysis is a simplified integral breadth method where both size-induced and strain-induced broadening are deconvoluted by considering the peak width as a function of 2θ [14]. In the present study, W-H analysis is employed for estimating crystallite size and lattice strain. Although X-ray profile analysis is an average method, they still hold an unavoidable position for grain size determination, apart from TEM micrographs.

In this present work, a comparative evaluation of the mean particle size of ZnO nanoparticles obtained from direct TEM measurements and from powder X-ray diffraction (XRD) peak broadening is reported. The strain associated with the as-prepared and annealed ZnO samples at 450°C due to lattice deformation was estimated by a modified form of W-H, namely, uniform deformation model (UDM). The other modified models, such as uniform deformation stress model (UDSM) and uniform deformation energy density model (UDEDM), gave an idea of the stress–strain relation and the strain as a function of energy density 'u'. In UDM, the isotropic nature of the crystal is considered, whereas UDSM and UDEDM assume that the crystals are of an anisotropic nature. The strain associated with the anisotropic nature of the hexagonal crystal is compared and plotted with the strain resulting from the interplanar spacing. We report such investigations on ZnO nanoparticles synthesized by coprecipitation method in this paper laconically and qualitatively.

Results and discussion
XRD analysis

The XRD pattern of the ZnO powder as shown in Figure 1 is having a wurtzite structure. No extra diffraction peaks corresponding to Zn, $Zn(OH_2)$, or other ZnO phases are detected, indicating that the pure ZnO nanoparticles are crystalline in nature. The peaks' intensity is sharp and narrow, confirming that the sample is of high quality with good crystallinity and fine grain size. Using XRD data, lattice parameters were calculated ($a = 3.2491$ Å and $c = 5.2063$ Å).

Crystalline size and strain

The significance of the broadening of peaks evidences grain refinement along with the large strain associated with the powder. The instrumental broadening (β_{hkl}) was corrected, corresponding to each diffraction peak of ZnO material using the relation:

$$\beta_{hkl} = \left[(\beta_{hkl})^2_{\text{Measured}} - (\beta_{hkl})^2_{\text{Instrumental}} \right]^{1/2}. \qquad (1)$$

The average nanocrystalline size was calculated using Debye-Scherrer's formula:

$$D = \frac{K\lambda}{\beta_{hkl}\cos\theta}, \qquad (2)$$

where D = crystalline size, K = shape factor (0.9), and λ = wavelength of Cuk_α radiation. From the calculations, the average crystalline size of the ZnO nanoparticles is 27 nm.
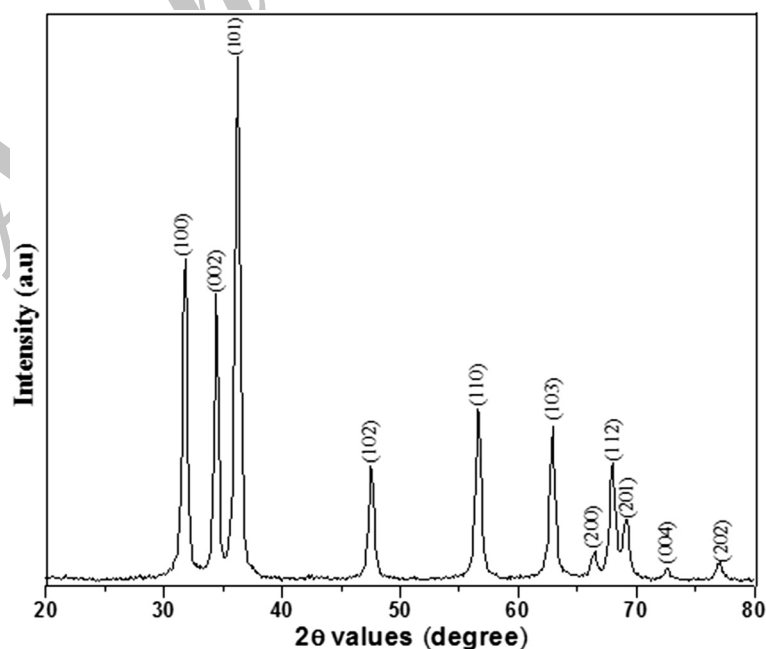

Figure 1 X-ray diffractogram of ZnO.

The strain induced in powders due to crystal imperfection and distortion was calculated using the formula:

$$\varepsilon = \frac{\beta_{hkl}}{4\tan\theta}. \tag{3}$$

From Equations 2 and 3, it was confirmed that the peak width from crystallite size varies as $\frac{1}{\cos\theta}$ strain varies as $\tan\theta$.

Assuming that the particle size and strain contributions to line broadening are independent to each other and both have a Cauchy-like profile, the observed line breadth is simply the sum of Equations 2 and 3.

$$\beta_{hkl} = \frac{K\lambda}{D\cos\theta} + 4\varepsilon\tan\theta \tag{4}$$

By rearranging the above equation, we get

$$\beta_{hkl}\cos\theta = \frac{K\lambda}{D} + 4\varepsilon\sin\theta. \tag{5}$$

The above equations are W-H equations. A plot is drawn with $4\sin\theta$ along the x-axis and $\beta_{hkl}\cos\theta$ along the y-axis for as-prepared ZnO nanoparticles as shown in Figure 2. From the linear fit to the data, the crystalline size was estimated from the y-intercept, and the strain ε, from the slope of the fit. Equation 5 represents the UDM, where the strain was assumed to be uniform in all crystallographic directions, thus considering the isotropic nature of the crystal, where the material properties are independent of the direction along which they are measured. The uniform deformation model for ZnO nanoparticles is shown in Figure 2.

Uniform deformation stress and uniform deformation energy density were taken into account; the anisotropic nature of Young's modulus of the crystal is more realistic [14-16]. The generalized Hook's law referred to the strain, keeping only the linear proportionality between the stress and strain, i.e., $\sigma = E$. Here, the stress is proportional to the strain , with the constant of proportionality being the modulus of elasticity or Young's modulus, denoted by E. In this approach, the Williamson-Hall equation is modified by substituting the value of ε in Equation 5; we get

$$\beta_{hkl}\cos\theta = \frac{K\lambda}{D} + 4\sin\theta\sigma/E_{hkl}. \tag{6}$$

E_{hkl} is Young's modulus in the direction perpendicular to the set of the crystal lattice plane (hkl).

The uniform stress can be calculated from the slope line plotted between $4\sin\theta/E_{hkl}$ and $\beta_{hkl}\cos\theta$, and the crystallite size D, from the intercept as shown in Figure 3. The strain can be measured if E_{hkl} of hexagonal ZnO nanoparticles is known. For samples with a hexagonal crystal phase, Young's modulus E_{hkl} is related to their elastic compliances S_{ij} as [12,13]

$$E_{hkl} = \frac{\left[h^2 + (h+2k)^2/3 + (al/c)^2\right]^2}{S_{11}\left(h^2 + (h+2k)^2/3\right) + S_{33}(al/c)^4 + (2S_{13}+S_{44})\left(h^2 + (h+2k)^2/3(al/c)^2\right)}, \tag{7}$$

where S_{11}, S_{13}, S_{33}, and S_{44} are the elastic compliances of ZnO, and their values are 7.858×10^{-12}, 2.206×10^{-12}, 6.940×10^{-12}, and 23.57×10^{-12} $m^2 N^{-1}$, respectively [17]. Equation 7 represents the UDSM. Plotting the values of $\beta_{hkl}\cos\theta$ as a function of $4\sin\theta/E_{hkl}$, the uniform deformation
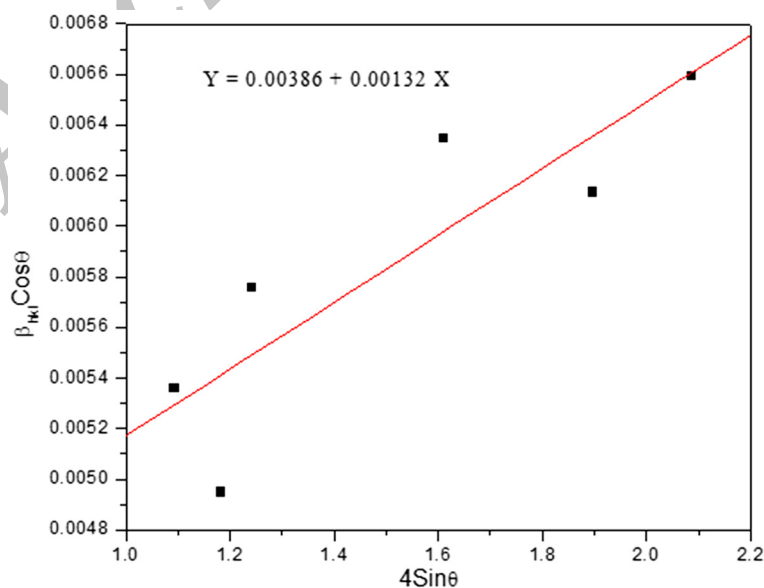

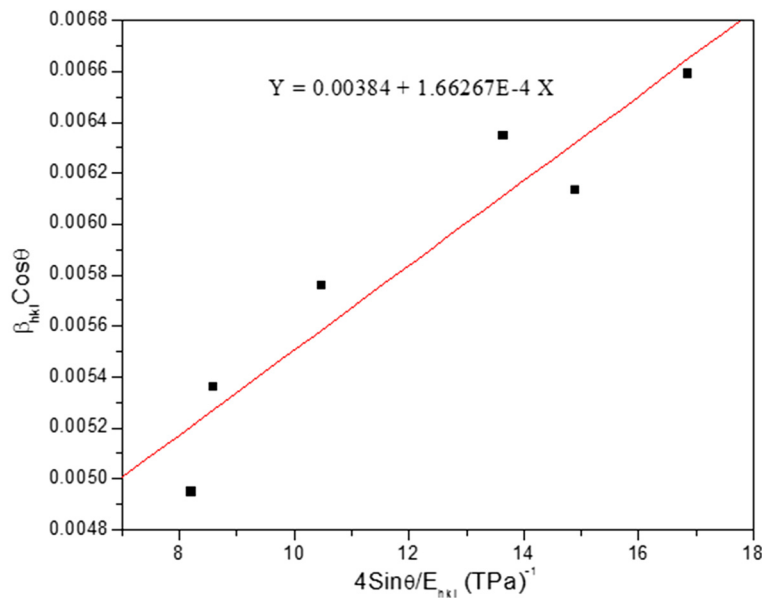**Figure 2** Plot of $\beta_{hkl}\cos\theta$ vs $4\sin\theta$ of ZnO sample.

Figure 3 Plot of $\beta_{hkl} \cos\theta$ vs $4\sin\theta/E_{hkl}$ of ZnO sample.

stress can be calculated from the slope of the line and from lattice strain. UDSM for annealed ZnO nanoparticles is shown in Figure 3.

In Equation 5, we have considered the homogeneous isotropic nature of the crystal. However, in many cases, the assumption of homogeneity and isotropy is not fulfilled. Moreover, all the constants of proportionality associated with the stress–strain relation are no longer independent when the strain energy density u is considered. According to Hooke's law, the energy density u (energy per unit volume) as a function of strain is $u = \varepsilon^2 E_{hkl}/2$. Therefore, Equation 6 can be modified to the form, where u is the energy density (energy per unit volume):

$$\beta_{hkl} cos\theta = \frac{K\lambda}{D} + \left(4\sin\theta (2u/E_{hkl})^{1/2} \right). \tag{8}$$

The uniform deformation energy density (UDEDM) can be calculated from the slope of the line plotted between $\beta_{hkl} \cos\theta$ and $4\sin\theta (2/E_{hkl})^{1/2}$. The lattice strain can be calculated by knowing the E_{hkl} values of the sample. W-H
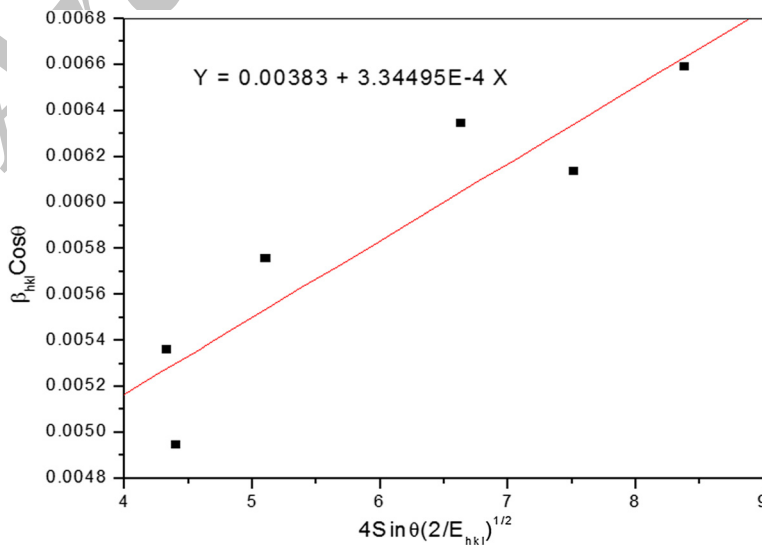

Figure 4 Plot of $\beta_{hkl} \cos\theta$ vs $4\sin\theta (2/E_{hkl})^{1/2}$ of ZnO sample.
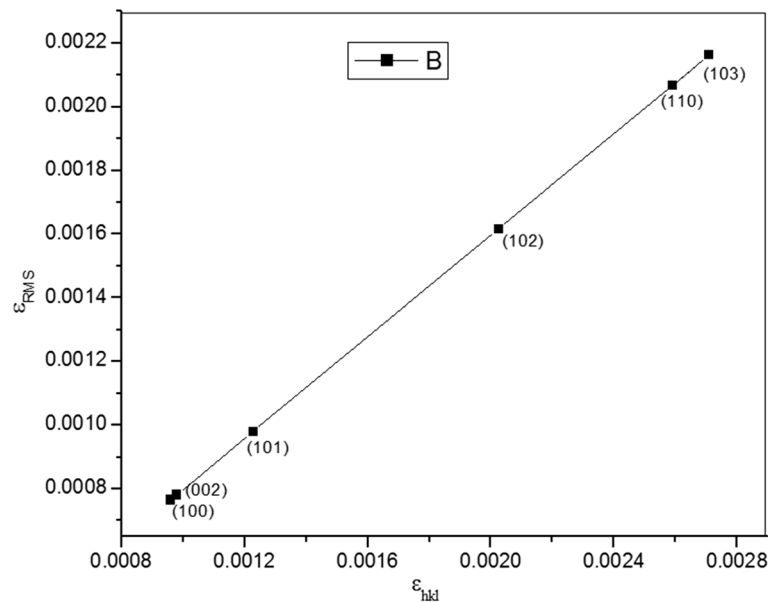
Figure 5 ε_{RMS} vs ε_{hkl} of ZnO sample.

equations modified assuming UDEDM and the corresponding plot are shown in Figure 4. From Equations 6 and 8, the energy density and the stress can be related with UDSM and UDEDM, but approaches are different, based on the assumption of uniform deformation stress, according to Equation 6. The assumption of uniform deformation energy is as per Equation 8, even though both models consider the anisotropic nature of the crystallites. From Equations 6 and 8, the deformation stress and deformation energy density are related as $u = \sigma^2/E_{hkl}$. It may be noted that though both Equations 6 and 8 are taken into account in the anisotropic nature of the elastic constant, they are essentially different. This is because in Equation 3, it is assumed that the deformation stress has the same value in all crystallographic directions allowing u to be anisotropic, while Equation 8 is developed assuming the deformation energy to be uniform in all crystallographic directions treating the deformation stress σ to be
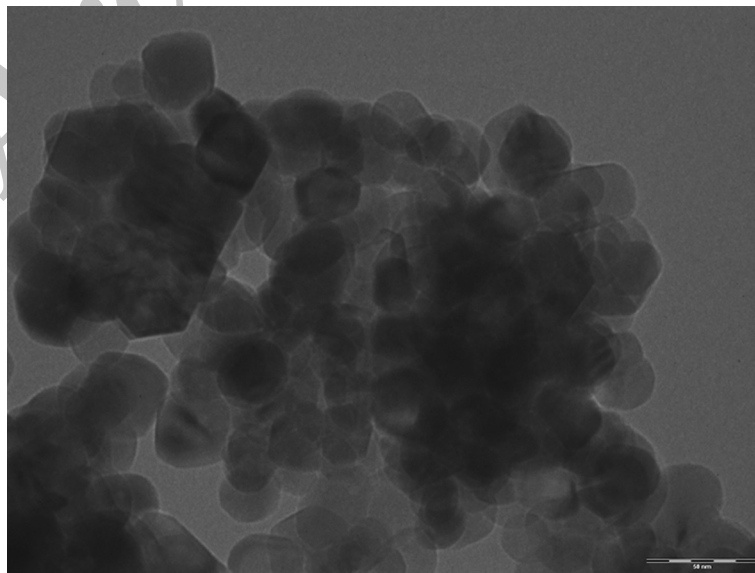

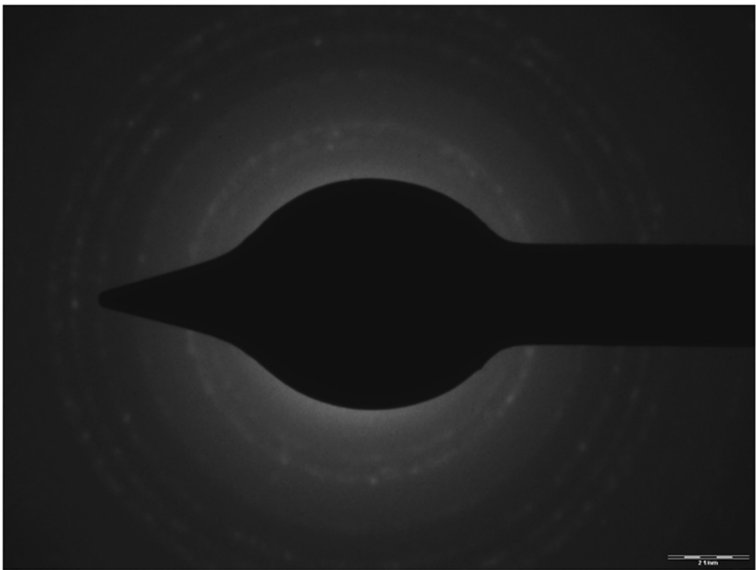**Figure 6** TEM image of ZnO nanopowders.

Figure 7 SAED patterns of ZnO nanopowders.

anisotropic. Thus, it is clear that from Williamson-Hall plots using Equations 6 and 8, a given sample may result in different values for lattice strain and crystallite size. For a given sample, Williamson-Hall plots may be plotted using Equations 1 to 8, and the most suitable model may be chosen as the one, which results in the best fit of the experimental data. A comparison of the three evaluation procedures for the nanocrystalline ZnO sample is possible from the analysis of Figure 4. The scattering of the points away from the linear expression is lesser for Figure 2 as compared with Figures 3 and 4. Further, the average crystallite sizes are estimated from the *y*-intercept of the graphs shown in Figures 2, 3, and 4, i.e., 35, 36, and 36 nm, respectively. It can be noted that the values of the average crystallite size obtained from the UDEDM, UDM, and UDSM are in good agreement with the results of the TEM analysis. Thus, it may be concluded that these models are more realistic in the present case. The values of crystallites obtained from the three models are in good agreement with the values obtained from Scherrer's formula and TEM. Our results are more appropriate than the reported literature [18]. As far as authors are concerned, a detailed study using these models on the ZnO-synthesized sample annealed at 450°C is not reported yet. This study throws some more light and reveals importance of models in the determination of particle size of ZnO nanomaterials. We suggest that these three models are the best models for the evaluation of the crystallite size of ZnO nanoparticles. This is in agreement with the results of Rosenberg et al. that for metallic samples with cubic structures, the uniform deformation energy model is suitable [19]. In our case, all three models are found suitable for the determination of crystallite size.

The root mean square (RMS) lattice strain, $< \varepsilon_{RMS} >= (2/\pi)^{1/2}(\Delta d/d_0)$, estimated [20] from the observed variation in the interplanar spacing values is plotted against those estimated using the uniform deformation energy density model, E_{hkl} as shown in Figure 5. Here, d and d_0 represent the observed and ideal interplanar spacing values, respectively. Figure 5 shows the plot of RMS strain against variation in the interplanar spacing for the uniform deformation energy density model. Theoretically, if the strain values agree, all the points should lie on a straight line with an angle of 45° to the *x*-axis. The RMS strain linearly varies with the strain calculated from the interplanar spacing, which attributed to no discrepancy on the (hkl) planes in the nanocrystalline nature [21]. Lattice strain in the nanocrystalline ZnO nanoparticles may arise from the excess volume of grain boundaries due to dislocations.

Table 1 Geometric parameters of the ZnO nanoparticles

Scherrer's method	W-H method										TEM
	UDM		USDM			UDEDM				particle size (nm)
D (nm)	*D* (nm)	$\varepsilon \times 10^{-4}$	*D* (nm)	Σ (MPa)	$\varepsilon \times 10^{-4}$	*D* (nm)	*u* (kJm^{-3})	σ (MPa)	$\varepsilon \times 10^{-4}$	
27	35	0.00131	36	166	0.00130	36	67	100.5	0.00113	50

In TEM, electron beams focused by electromagnetic lines are transmitted through a thin sample of ZnO nanopowders. Figures 6 and 7 display the TEM image and selected area electron diffraction (SAED) pattern of annealed ZnO nanoparticles. The mean size estimated from the TEM image is about 50 nm and clearly indicates that the annealed ZnO nanoparticles are crystalline with a wurtzite structure, and no other impurities were observed. This is in close agreement with the results obtained from powder XRD data. In addition, the rings with a dotted pattern in SAED confirm the wide size distribution of ZnO nanoparticles.

Young's modulus (E) is calculated using Equation 7 for ZnO nanoparticles and is approximately 127 GPa, which is in agreement with the bulk ZnO [22]. Table 1 summarizes the geometric parameters of ZnO nanoparticles obtained from Scherrer's formula, various modified forms of W-H analysis, and TEM results. By comparing the values of average crystallite size obtained from UDM, UDSM, and UDEDM, it was found that the values are almost similar, implying that the inclusion of strain in various forms has a very small effect on the average crystallite size of ZnO nanoparticles. However, the average crystallite size obtained from Scherrer's formula and W-H analysis shows a small variation; this is because of the difference in averaging the particle size distribution. The values of strain from each model are calculated by considering Young's modulus E_{hkl} to be 127 GPa. The average crystallite size and the strain values obtained from the graphs plotted for various forms of W-H analysis, i.e., UDM, UDSM, and UDEDM, were found to be accurate, comparable, and reasonable, as their entire preferred high intensity points lay close to the linear fit.

Conclusions

ZnO nanoparticles were synthesized by coprecipitation process and characterized by powder XRD and TEM. The line broadening of ZnO nanoparticles due to the small crystallite size and strain was analyzed by Scherrer's formula. The size and strain contributions to line broadening were analyzed by the method of Williamson and Hall using uniform deformation, uniform deformation stress, and uniform deformation energy density models. The uniform deformation energy density model models the strain most appropriately. A modified W-H plot has been worked out and accepted to determine the crystallite size and strain-induced broadening due to lattice deformation. With the assumption of a hexagonal anisotropic crystalline nature, the RMS lattice strain differs from the strain calculated from UDSM and UDEDM. TEM image of annealed ZnO nanoparticles reveals the nanocrystalline nature, and their particle size is found to be 50 nm. The three modified forms of W-H analysis were helpful in determining the strain, stress,

and energy density value with a certain approximation, and hence, these models are highly preferable to define the crystal perfection. The value of crystallite size calculated from the W-H analysis is in agreement with that of the average crystallite size measured from TEM.

Methods

Sample preparation

ZnO nanoparticles were prepared by the reaction of Zn^{2+} and OH^- in an alcoholic medium (methanol) at low temperature. Zinc acetate dehydrate $Zn(CH_3COO)_2 \cdot 2H_2O$, potassium hydroxide (KOH), and methanol are used as starting materials. In this procedure, pure ZnO and two solutions, one containing zinc acetate dehydrate dissolved in 100 ml methanol and the other containing KOH in 100 ml methanol, were prepared and aided by magnetic stirring while heating at 52°C for 2 h. The KOH solution was added to the solution containing $Zn(CH_3COO)_2 \cdot 2H_2O$ with constant stirring while heating at 52°C for 2 h; it was aged for 2 days. The precipitate which formed was separated from the solution by filtration, washed several times with distilled water and absolute ethanol, and then dried in air at 127°C to obtain ZnO nanocrystalline powders. The nanocrystalline sample was annealed at 450°C in air for 8 h.

Characterization

XRD and TEM were used to obtain the textural parameters like size, shape, and crystal structure in order to understand the enhanced properties of as-prepared and annealed ZnO nanoparticles. XRD was performed by powder X-ray diffraction (model: PW-3710; FEI Co., Hillsboro, OR, USA) using CuKα radiation ($\lambda = 1.5406$ Å). For TEM analysis, it was used to examine the morphology of the annealed ZnO nanoparticles. Crystallite size and lattice strain were determined using Scherrer's formula and W-H analysis.

Author details
[1]Department of Physics, Materials Research Laboratory, Dr. Babasaheb Ambedkar Marathwada University, Aurangabad 431 004, India. [2]Centre for Materials for Electronics Technology, HCL (PO), Cherlapally, Hyderabad 500 051, India.

References
1. Harbour, JR, Hair, ML: J. Phys. Chem. **83**, 652 (1979)
2. Mitra, P, Chatterjee, A, Maiti, H: Mater. Lett. **35**, 33 (1998)
3. Gupta, TK: J. Am. Ceram. Soc. **73**, 1817 (1990)
4. Dijken, AV, Mulenkamp, EA, Vanmaekelbergh, D, Meijerink, A: J. Lumin. **90**, 123 (2000)
5. Hotchandani, S, Kamat, PV: J. Electrochem. Soc. **113**, 2826 (1991)

6. Sakohapa, S, Tickazen, LD, Anderson, MA: J. Phys. Chem. **96**, 11086 (1992)
7. Ramakanth, K: Basics of X-ray Diffraction and its Application. I.K. International Publishing House Pvt. Ltd., New Delhi (2007)
8. Ungar, T: J. Mater. Sci. **42**, 1584 (2007)
9. Suryanarayana, C: Mechanical Alloying and Milling. Marcel Dekker, New York (2004)
10. Cullity, BD, Stock, SR: Elements of X-ray diffraction, 3rd ed. Prentice Hall Publication, India (2001)
11. Rietveld, HM: Acta Crystallogr. **22**, 151 (1976)
12. Balzar, D, Ledbetter, H: J. Appl. Crystallogr. **26**, 97 (1993)
13. Warren, BE, Averbach, BL: J. Appl. Phys. **21**, 595 (1950)
14. Suryanarayana, C, Grant Norton, M: X-ray Diffraction: A Practical Approach. Springer, New York (1998)
15. Adachi, S: Handbook on Physical Properties of Semiconductors. Springer, New York (2004)
16. Zhang, J, Zhang, Y, Xu, KW, Ji, V: Sol. State Commun. **139**, 87 (2006)
17. Nye, JF: Physical Properties of Crystals: Their Representation by Tensors and Matrices. Oxford, New York (1985)
18. Yogamalar, R, Srinivasan, R, Vinu, A, Ariga, K, Bose, AC: Sol. State Commun. **149**, 1919 (2009)
19. Rosenberg, Yu, Machavariant, VSh, Voronel, A, Garber, S, Rubshtein, A, Frenkel, AI, Stern, EA: J Phys. Cond. Mater. **12**, 8081 (2000)
20. Dapiaggi, M, Geiger, CA, Artioli, G: Am. Miner. **90**, 506 (2005)
21. Biju, V, Sugathan, N, Vrinda, V, Salini, SL: J. Mater. Sci. **43**, 1175 (2008)
22. Weber, MJ: Handbook of Optical Materials. CRC Press, London (2003)